Solar Energy Materials & Solar Cells 92 (2008) 1091–1098

Contents lists available at ScienceDirect

Solar Energy Materials & Solar Cells

journal homepage: www.elsevier.com/locate/solmat

# Plasma-enhanced chemical vapour-deposited silicon nitride films; The effect of annealing on optical properties and etch rates

Daniel N. Wright [a,*], Erik S. Marstein [a], Atle Rognmo [b], Arve Holt [a]

[a] Section for Renewable Energy, Institute for Energy Technology, Postboks 40, 2027 Kjeller, Norway
[b] Norwegian Defence Research Establishment, Instituttveien 20, 2027 Kjeller, Norway

ARTICLE INFO

*Article history:*
Received 3 March 2008
Accepted 13 March 2008
Available online 7 May 2008

*Keywords:*
PECVD
Silicon nitride
Annealing
Optical properties
Etch rate

ABSTRACT

The optical properties and etch rates of silicon nitride ($SiN_x$:H) deposited by plasma-enhanced chemical vapour deposition (PECVD) and their correlation with bond concentrations have been studied. By varying the silane-to-total gas ratio, films with refractive index ($n$) between 1.92 and 3.00 were deposited. Higher $n$ films had increased absorption and decreased etch rates. Annealing the samples at different temperatures revealed that all films were thermally stable up to 750 °C, above which all experienced a rise in $n$, attributed mainly to mass densification. The etch rate correlated well the N–H bond concentration for both annealed and as-deposited films.



## 1. Introduction

Hydrogenated amorphous silicon nitride ($SiN_x$:H) fabricated by plasma-enhanced chemical vapour deposition (PECVD) has become the industry standard for application of anti-reflective coatings (ARC) on screen-printed multicrystalline (mc) silicon (Si) solar cells [1]. When using silane ($SiH_4$) and ammonia ($NH_3$) as process gases, the refractive index ($n$) of the deposited film can be varied from about 1.8 to 3.3 [2,3] by adjusting the gas flow ratio

$$R_G = \frac{\Phi_{SiH_4}}{\Phi_{SiH_4} + \Phi_{NH_3}} \quad (1)$$

where $\Phi_{SiH_4}$ and $\Phi_{NH_3}$ are the $SiH_4$ and $NH_3$ gas flows, respectively. This renders PECVD $SiN_x$:H interesting for multilayer ARCs [4–6], which consist of a stack of two or more films with varying $n$, decreasing from the bottom to the top of the stack.

Screen-printed mc-Si solar cells must undergo a final firing step to allow metal pastes to etch through the $SiN_x$:H and form a good ohmic contact with the underlying Si. For this purpose it is vital for the optical performance of the cell that the behaviour of the PECVD $SiN_x$:H upon annealing is known. The same argument holds for applying $SiN_x$:H as a diffusion barrier mask, where the $SiN_x$:H film must withstand long annealing treatments and still be possible to remove by a subsequent etch.

In this paper we have studied the effect of $R_G$ on the optical properties of PECVD $SiN_x$:H films, which have been characterised by spectroscopic ellipsometry. The Si–N, Si–H and N–H bond concentrations have been estimated using Fourier transform infrared transmission spectroscopy (FTIR). For this purpose we have developed an asymmetric representation of the extinction coefficient ($k$), which proved to give good fits against experimental data. Etch rates in dilute hydrogen fluoride (HF) solution, which is commonly used in the semiconductor industry, were also determined.

## 2. Experimental

### 2.1. Sample preparation

The samples used in this study were double side polished p-type polished Cz-Si. Prior to loading in the PECVD chamber, the samples received a 1 min dip in 5% HF solution, followed by a 3 min rinse in de-ionised water and blow-drying in nitrogen.

### 2.2. $SiN_x$:H deposition

$SiN_x$:H films were deposited in a vertically mounted parallel plate PECVD system with an electrode spacing of 30 mm. Plasma excitation was achieved using a 13.56 MHz generator set to deliver a plasma power density of 16.8 mW cm$^{-2}$. The temperature and pressure were 300 °C and 0.5 Torr, respectively. The gas flows of $SiH_4$ and $NH_3$ were controlled by mass flow controllers enabling the variation in $R_G$ between 0.095 and 0.500, while keeping the total gas flow constant at 210 sccm.

* Corresponding author. Tel.: +47 63806463.
*E-mail address:* danielnw@ife.no (D.N. Wright).

0927-0248/$ - see front matter © 2008 Elsevier B.V. All rights reserved.
doi:10.1016/j.solmat.2008.03.013

After deposition each wafer was split into nine parts. The middle part was kept as-deposited while the surrounding eight were annealed in a belt furnace with temperatures ranging from 550 °C to 900 °C in 50 °C increments. The total anneal time was about 10 s.

The etch rate was determined by subsequent dipping of the samples in 5% HF for 10 s between each ellipsometry measurement, as described below.

### 2.3. Characterisation

#### 2.3.1. Ellipsometry

Ellipsometry is a commonly used technique for characterising optical dispersion relationships, $\tilde{n}(\lambda) = n(\lambda) + ik(\lambda)$, where $\lambda$ is the wavelength, while $n(\lambda)$ and $k(\lambda)$ are the spectral refractive index and extinction coefficient of a material, respectively. In this study, ellipsometry measurements were performed using a vertical variable angle spectroscopic ellipsometer (V-VASE) from Woollam & Co. The measurements were made in the 250–800 nm range in 10 nm increments. Angles of incidence of 65°, 70° and 75° were used for the characterisation of as-deposited and annealed films, while a single angle of 70° was used for the etch rate determination experiment.

The dispersion relationships and film thicknesses were estimated by fitting an appropriate model to the ellipsometric data using the WVASE32 software package from Woollam & Co. The model used is shown in Fig. 1. It consists of a Si substrate covered by a thin silicon oxide ($SiO_2$) layer, where dispersion relationships for both materials are taken from the software database. The purpose of the $SiO_2$ layer is to take into account the possible formation of a native oxide in the preparation process. On top of the $SiO_2$ layer is the $SiN_x$:H layer to be characterised, as discussed below. On top of the $SiN_x$:H layer there was added a roughness layer which was modelled by a Bruggemann effective medium approximation consisting 50% voids and 50% of the underlying $SiN_x$:H material [7,8].

The dispersion relationships were parameterised using the Tauc–Lorentz oscillator formalism developed by Jellison and Modine [9], which has previously been used to successfully characterise $SiN_x$:H films [2,8,10] and is generally considered a good choice of model for weakly absorbing thin films. The formalism combines Tauc's expression for joint density of states with a Lorentz oscillator for a single transition [9], giving the complex part of the dielectric function, $\varepsilon_2$, the form

$$\varepsilon_2(E) = \begin{cases} \left[\dfrac{AE_0C(E-E_g)^2}{(E^2-E_0^2)^2 + C^2E^2}\dfrac{1}{E}\right] & E > E_g \\ 0 & E \leqslant E \end{cases} \quad (2)$$

where $A$ is an amplitude, $E_0$ is the peak transition energy, $C$ is a broadening term and $E_g$ is the optical band gap. Hence there is no need for a separate evaluation of $E_g$ when using this model. The real part of the dielectric function, $\varepsilon_1$, is deduced from $\varepsilon_2$ using Kramers–Kronig integration (see Ref. [9] for details).

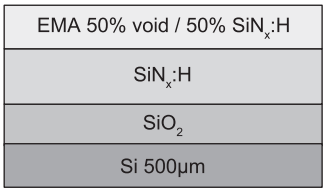


**Fig. 1.** The model used in this study to estimate the dispersion relationships and film thicknesses from ellipsometry measurements.

As the $n$ of thin films is very often measured using single-wavelength ellipsometry at $\lambda \approx 633$ nm, any referral to a numerical value of $n$ herein refers the value of $n(\lambda)$ at this wavelength.

#### 2.3.2. Bond concentrations estimated from FTIR spectroscopy

FTIR transmission spectroscopy is a commonly used, non-destructive tool for estimating the bond concentrations, [A–B], between atoms A and B in dielectric thin films, such as $SiN_x$:H [11,12].

The measurements were performed using a Spectrum GX Optica from Perkin-Elmer. The measurement range chosen for the wavenumber, $\omega$, was 300–7800 $cm^{-1}$. The measuring chamber was flushed with $N_2$ to minimise the signal from $CO_2$ and $H_2O$ in the ambient.

The bond concentrations were estimated by fitting an optical model to the FTIR measurements using the VWASE32 software. The structural model is shown in Fig. 1, where the thicknesses for each layer was taken from the ellipsometry measurements and $n(\omega)$ of the $SiN_x$:H layer was represented by Cauchy power series with $n_0$, $B$ and $C$ as fitting parameters as follows:

$$n(\omega) = n_0 + B\omega^2 + C\omega^4 \quad (3)$$

This is a commonly used parameterisation used for PECVD $SiN_x$:H films [13].

The absorption peaks of each bond were modelled by representing $k(\omega)$ by mathematical functions with peak positions given in Ref. [14] and summarised in Table 1. The Si–H bond was represented as a single Gaussian, as this was found to give a better fit than convoluting individual peaks listed in Table 1. The $Si–N_I$ and $Si–N_{III}$ peaks were represented by Gaussians while the asymmetric $Si–N_{II}$ and $N–H_{II}$ peaks were found to be best represented by

$$k(\omega) = \frac{A \times t^{p/2}}{t^{p/2} + (|\omega - \omega_c|^{p/2}/t^{p/2})} \times \left(b_1 + \frac{b_2 - b_1}{1 + \exp((\omega_c - \omega) \times r)}\right) \quad (4)$$

where the left-hand side of the multiplier is a modified Cauchy distribution function while the right-hand side is a modified Sigmoid function. The Cauchy part of Eq. (4) comprises of the peak position, $\omega_c$, the half-width at half-maximum, $t$, the peak height, $A$, and a power parameter, $p$. The first three are fairly self-explanatory. The power parameter allows adjustment of the curve around the peak. Low values will lower the slope and sharpen the peak while high values will increase the slope and flatten the

**Table 1**
Table listing the name, description peak positions ($\omega_{peak}$) and proportionality factors ($K_{(A–B)}$) of the bond peaks that were analysied in this paper

| Name | Description | $\omega_{peak}$ ($cm^{-1}$) | $K_{(A–B)}$ ($\times 10^{19}$ $cm^{-2}$) |
|---|---|---|---|
| Si–H | | | |
| $Si–H_I$ | $H–Si–Si_3$ | 2005 | 7 |
| $Si–H_{II}$ | $H_2–Si–Si_2$ | 2065 | 11 |
| $Si–H_{III}$ | $H–Si–NSi_2$ | 2082 | 17 |
| $Si–H_{IV}$ | $H–Si–SiN_2/H_2–Si–NSi$ | 2140 | 11 |
| $Si–H_V$ | $H_2–Si–N_2$ | 2175 | 40 |
| $Si–H_{VI}$ | $H–Si–N_3$ | 2220 | 20 |
| N–H | | | |
| $N–H_I$ | N–H stretch | 3335 | 12 |
| $N–H_{II}$ | N–H wag rock | 1175 | 2 |
| Si–N | | | |
| $Si–N_I$ | Si–N | 790 | 1.5 |
| $Si–N_{II}$ | $N–Si_3$ asymmetric | 850 | 1.5 |
| $Si–N_{III}$ | Si–N | 1020 | 1.5 |

The values are taken from Ref. [14].